Transfer of Thiolated DNA Staples from DNA Origami Nanostructures to Self-Assembled Monolayer Passivated Gold Surfaces: Implications for Interfacial Molecular Recognition

Qufei Gu[†], Yehan Zhang[‡], Huan H. Cao[‡], Songtao Ye[§], and Tao Ye*[,‡]

[†]Materials and Biomaterials Science and Engineering, [‡]Chemistry and Chemical Biology and [§]Quantitative and Systems Biology, University of California, Merced, Merced, California, 95343, United States

ABSTRACT: We show that thiolated strands displayed on a DNA origami nanostructure can be transferred to a gold surface when the DNA origami tile is deposited onto a self-assembled monolayer (SAM) passivating the surface. Spatial statistical analysis revealed the ink molecule transfer yield to be 70%, comparable to the highest yield achieved with existing DNA-nanostructure-based nanoimprinting methods. The surface passivation reduces nonspecific adsorption and allows high resolution, label-free characterization of the transferred spatial patterns. Therefore, our method offers a pathway toward forming complex single molecule nanoarrays for elucidating the structure-function relationships of enzyme cascades and interfacial molecular recognition.

KEYWORDS: DNA origami nanostructure, nanoimprinting, atomic force microscope (AFM), DNA-surface interaction, spatial patterns

INTRODUCTION

A variety of methods have been developed to pattern biological molecules on solid surfaces for a diverse range of applications, from multiplexed sensing, microarrays and nanoarrays,[1] to probing and controlling cell adhesion and signaling.[2-3] An emerging need is to arrange single biomolecules in prescribed geometry with separations that are on the order of ten nanometers or smaller.[4] This new level of precision in patterning biomolecules will help to elucidate the structure-function relationship of biological systems such as multi-enzyme cascades[5] and molecular recognition at cell surfaces,[6-7] as the positions of individual enzyme/receptors molecules need to be precisely defined to understand and control how these molecules work together to enable emergent functions that are not available to isolated molecules or uncontrolled aggregates. Moreover, recent studies revealed that the spatial patterns of single receptor molecules on surfaces may have a major impact on the performance of DNA biosensors and other biotechnological devices,[8-10] further underscoring the need to pattern single molecules to gain a molecular level understanding of interfacial molecular recognition and improve the performance of these devices.

While scanning probe microscope-based techniques, such as single molecule cut and paste[11] and single molecule nanografting,[12] can pattern single or few molecules on surfaces, achieving a resolution of 10 nm or better remains an unresolved challenge. Moreover, the throughput of these serial approaches remains too limited for large scale applications. DNA origami nanostructure offers a promising bottom-up route to patterning single molecules in a parallel fashion.[13-15] Hundreds of oligonucleotides (staples) can bind to specific regions of a long DNA (scaffold) and fold it into a designed 2D shape that is about 100 nm in size. The shape can serve as a breadboard that display single molecules of nucleic acids,[16] proteins,[17-19] gold nanoparticles,[20-21] quantum dots,[22] and other polymers[23] in arbitrary arrangements with nanometer or even subnanometer precision.[18-19] Despite the appeals, the DNA origami nanostructures often denature outside a narrow range of pH, buffer ionic strength and temperature.[24] Although different stabilization strategies such as tuning buffer conditions, covalent crosslinking and coating or encapsulation have been developed, the stability of the DNA nanostructures is highly dependent on structure design and functionalities added to the structure, which may hinder the accessibility of single molecule patterns to target molecules.[25-27]

An alternative way to improve the stability while maintaining the accessibility of single molecule patterns is to use DNA origami as a carrier to directly transfer the patterns to the substrate. Gállego et al. showed that DNA origami nanostructure can serve as a nanoscale stamp that transfers thiolated staples (ink molecules) to a bare gold surface due to the affinity of thiolate groups on gold.[28] After removing other DNAs through denaturing, passivating the gold surface with another thiol, oligonucleotide-functionalized gold nanoparticles (AuNPs) were captured by the surface immobilized ink molecules. A fraction of these gold nanoparticles was observed to assume the geometrical arrangement of ink molecules on the DNA origami stamp. However, most of the AuNPs were bound to locations that do not correspond to the binding sites of ink molecules, suggesting that the fidelity of this nanopatterning approach remains low. The origin of the low fidelity remains unclear. The molecules "immobilized" by gold-thiol interactions are in fact quite mobile when the surface coverage of the thiol molecules is low.[29] Indeed, previous studies that deposited thiolated oligonucleotides on a gold surface and then passivated the surface by "backfilling" with an inert thiol reported significant degrees of desorption and lateral diffusion.[30-31] In addition, not all transferred ink molecules can be labelled by the nanoparticles as the footprint of the AuNPs often exceeds the nearest distance between ink molecules.[28] Moreover, the AuNPs may non-specifically adsorb, further complicating the characterization of the single molecule patterns. Smith and coworkers developed an alternative method that first passivates the surface with a self-assembled monolayer (SAM) and then transfers ink molecules through amide coupling reaction with the SAM terminal groups.[32]

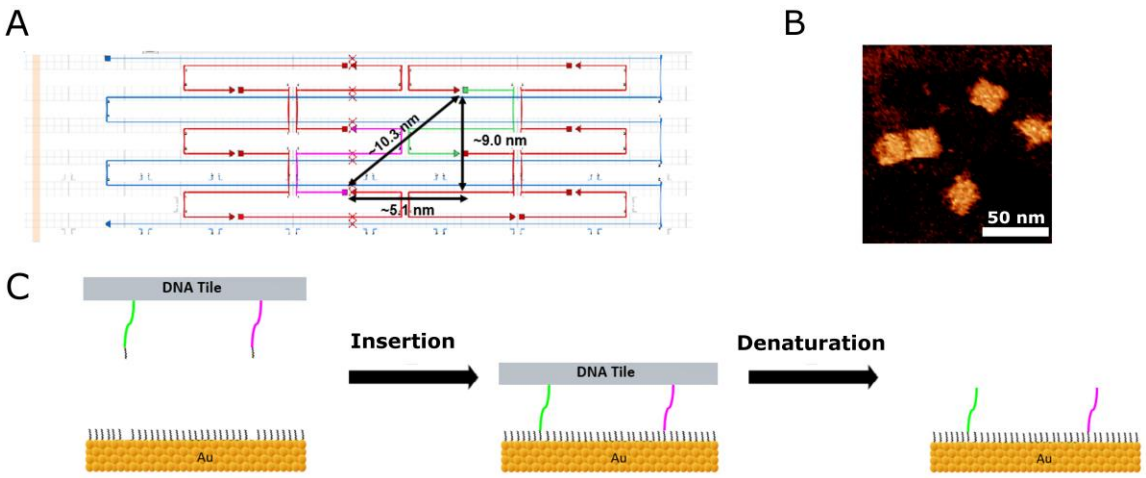

Figure 1. An overview of DNA-origami-guided pattern transfer. (A) CaDNAno diagram of DNA origami mini-tile with 12 staple strands on the square lattice. Two staples modified with thiol group at 5' terminus are highlighted in green and purple, respectively. (B) Representative AFM image of DNA mini-tile nanostructures. Scale bar is 50 nm. (C) DNA mini-tile carrying two thiolated staples with an extension protruding from the origami surface (green and purple) are deposited onto a MUDA SAM coated Au(111) surface. The frame of the DNA mini-tile is then denatured and rinsed out to expose the surface-tethered staples.

Streptavidin that binds to the biotin group on the ink molecule was used as the reporter. While this approach inhibits the lateral diffusion of the ink molecules transferred, the fraction of reporters that have formed the designed pattern remains small, possibly due to the low yield of the coupling reaction. Hence, existing efforts to create single molecule nanoarrays using DNA origami stamps are hampered by two intertwined challenges: an inadequate yield of ink molecule transfer, and the difficulty in quantifying the yield of the single molecule patterns.

RESULTS AND DISSCUSSION

Here we report a new DNA-origami-nanostructure-based nanoimprinting method that (1) allows atomic force microscopy (AFM) to directly characterize individual transferred DNA ink molecules without the use of any labels, (2) suppresses nonspecific adsorption and lateral diffusion of ink molecules. First, by depositing the folded DNA tiles possessing thiolated staples onto a SAM coated gold surface (Figure 1), we allowed the thiol anchors to be in close contact with the gold surface and have the opportunity to be inserted into the SAM to form covalent gold-thiol bonds, in a manner that is analogous to how thiolated ink molecules can be transferred from a polydimethylsiloxane stamp to a SAM surface.[33] Then the DNA origami frame was denatured to expose the spatial pattern (Figure 1C). Our previous studies showed that the lateral diffusion of oligonucleotides is effectively suppressed when they are inserted into a highly ordered SAM, helping to retain the fidelity of the single molecule pattern.[34] Compared to the bare gold surface used in previous studies, the use of highly ordered 11-mercaptoundecanoic acid (MUDA) SAM on an atomically smooth single-crystal Au(111) support allows us to minimize the impact of uncontrolled morphological (roughness) and compositional (defect density) heterogeneities, facilitating the transfer of ink molecules. Moreover, the SAM

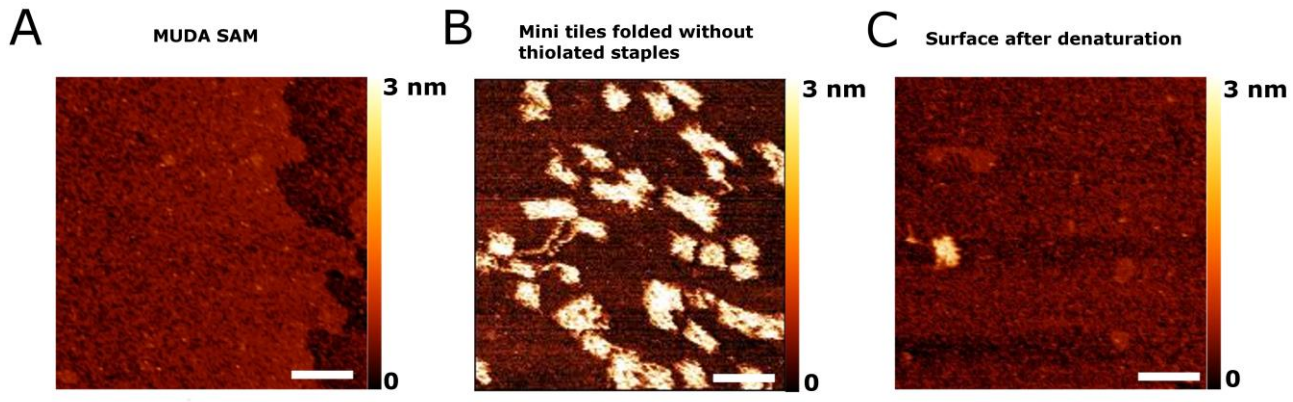

Figure 2. Surface deposition of DNA mini-tiles assembled without thiolated staples under Na^+. (A) Representative AFM image of the MUDA SAM surface before surface deposition. (B) Representative AFM image of DNA mini-tiles assembled without thiolated staples and deposited in 1 M NaAc. All the surfaces were rinsed with STAE buffer after 1 hr deposition. (C) AFM image of the MUDA SAM surface after denaturation.

allows the oligonucleotides to be pinned to the surface in the presence of divalent cations, allowing AFM to directly characterize the single molecule patterns with high resolution[34] and eliminating uncertainties and errors of imaging techniques that rely on labelling. Our previous studies showed that Ni^{2+} can strongly immobilize end-tethered DNA to MUDA SAM on gold.[9, 34] Other AFM studies of DNA typically require the DNA molecules be immobilized onto mica using divalent cations. The difference is that while ssDNAs are not immobilized enough to mica to be resolved by AFM, the MUDA SAM can routinely resolve end-tethered ssDNAs as protrusions due to two reasons. First, Ni^{2+} functions as a salt bridge that pins negatively charged DNA to the carboxylate surface. Second, covalent end tethering via thiol-gold interactions provides further immobilization beyond pure electrostatic immobilization. Although typically such protrusions are difficult to differentiate from nonspecifically adsorbed contaminants, our previous studies have established that the degree of nonspecific adsorption of DNA onto MUDA SAMs is very low under a monovalent cation buffer and almost all of these protrusions can be attributed to end-tethered thiolated DNA probes as over 85% of them can hybridize with a DNA target.[9]

We utilized various strategies to monitor the fidelity of nanoimprinting, suppress nonspecific adsorption, and promote transfer of ink molecules. To monitor the degree of nonspecific adsorption and the fidelity of ink transfer, we designed a DNA origami mini-tile "stamp" that can imprint a dimer, the simplest single molecule pattern. The mini tile is six helices wide and incorporates two staples containing single-stranded DNA extensions (highlighted in green and purple in Figure 1A) with a 5' end thiol termination (sequences in Table S1) that can bind to the gold surface. The distance between the two thiolated staples is ~10.3 nm (Figure 1A). It should be noted that, a short 10-base poly T extension (~3 nm) protruding from the origami surface allows the thiolated staples to rotate around their anchor points. However, these staples are not long enough to wrap around the edges of the tiles to insert into the SAM if the side of the ink molecule is facing up. To control the nonspecific adsorption and promote the ink transfer, we chose to perform nanoimprinting on a SAM that allows us to regulate DNA-surface interactions on demand by adjusting the buffer composition.[34] The highly ordered 11-mercaptoundecanoic acid (MUDA) SAM on an Au(111) surface repels DNAs in a neutral or basic solution that only contains monovalent cation as the carboxyl groups become ionized. DNAs are weakly adsorbed in a monovalent cation buffer with a high ionic strength, while they are strongly attracted toward the surface in the presence of divalent cations.

Apart from origami design and surface chemistry, surface deposition conditions of DNA origami nanostructures were also explored to reduce the nonspecific adsorption. Since the gold-thiol bond formation between the thiolated staples and the gold surface requires stable adsorption of DNA origami nanostructures on surface,[28] a conventional buffer containing divalent cations (1× TAE, 12.5 mM Mg^{2+}), which has been utilized to mediate the binding of even small DNAs to the surface,[35] was used for both origami folding and surface deposition. It should be noted that all surfaces were thoroughly rinsed with STAE (1× TAE, 200 mM Na^+) buffer after deposition. As depicted in Figure S2A, in the presence of Mg^{2+} only, application of unpurified DNA mini-tiles to the gold surface results in the adsorption of not only fully folded tiles but also partially folded intermediates (purple arrow), scaffolds (worm-like features, red arrow), and staples (dot-like features, green arrow arrow), as opposed to the clean and smooth MUDA SAM surface before deposition (Figure 2A). Note that the twin image features were caused by the double-tip imaging artifact. The high level of nonspecific adsorption of DNA origami components is not desirable as they can compete with folded DNA tiles for binding sites on surface. To reduce the number of nonspecifically adsorbed staples, we also attempted to purify the DNA origami nanostructures using Amicon column or gel purification (Figures S1and S2). However, despite of the decrease of the total number of staples, the purification steps were unable to reduce the density of nonspecifically adsorbed DNA staples to a negligible level, as evidenced by the high fraction of staples remaining on the surface (93% for Amicon column and 53% for gel purification, Figure S2) after purification, especially considering that Mg^{2+} can mediate strong attractive interaction of DNA to the surface.[35] Moreover, the purification steps reduced the density of DNA origami nanostructures, which is undesirable.

As DNA-surface interactions are weaker in a Na^+ buffer,[28, 36-38] which can also allow folding of DNA origami nanostructure to proceed,[39] we replaced Mg^{2+} with 1 M Na^+ in the folding solution to test

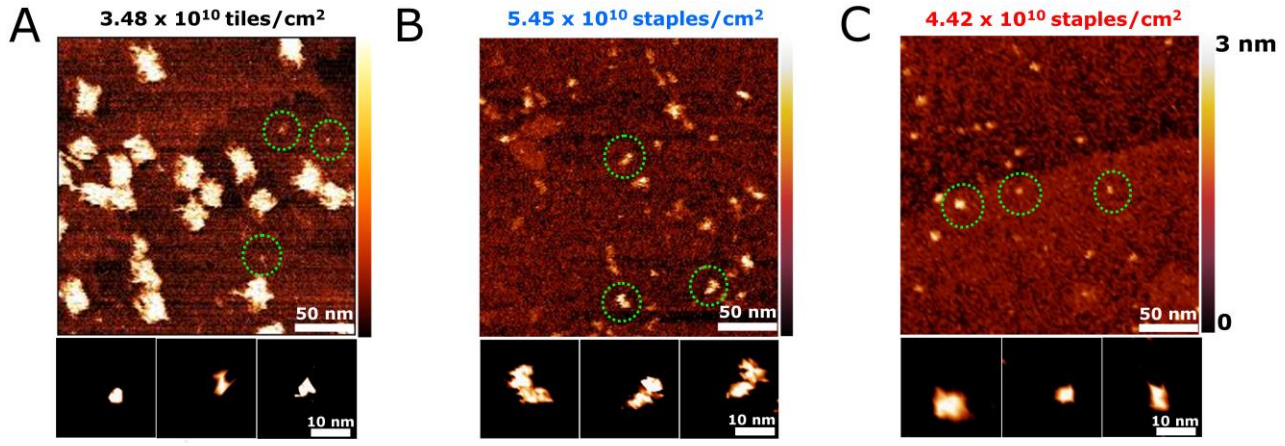

Figure 3. Surface deposition of DNA mini-tiles assembled with thiolated staples under Na^+. (A) Representative AFM image of DNA mini-tiles assembled and deposited in 1 M NaAc. All the surfaces were rinsed with STAE buffer after 1 hr deposition. (B) AFM image of the surface after denaturation. (C) AFM image of the surface prepared by direct insertion of thiolated staples into a MUDA SAM preassembled on Au(111) surface. Green circles highlight the surface-immobilized staples. The figures at the bottom are zoom-in images of the highlighted staples.

whether nonspecific adsorption could be suppressed. To examine the degree of nonspecific adsorption, we folded DNA origami nanostructures with only nonthiolated staples and deposited these unpurified and thiol-free DNA origami nanostructures onto a MUDA SAM in a buffer that contains 40 mM Tris-acetate, 1 mM EDTA and 1 M Na^+.[37] AFM shows that these DNA origami mini-tiles are adsorbed on the MUDA SAM due to weak nonspecific interactions between the DNA nanostructures and the SAM surface (Figure 2B). After denaturation using 100% formamide, the DNA origami features almost completely disappeared (Figure 2C). Moreover, no features associated with staples were observed. These results show that the interactions between staples and the surface are too weak in the monovalent cation buffer for the DNA staples to nonspecifically adsorb. Furthermore, unpurified DNA origami nanostructures folded with thiolated staples were successfully adsorbed with a high surface coverage of 3.5×10^{10} tiles/cm^2 ($3.5/100 \times 100$ nm^2) and fewer than 8% features corresponding to adsorbed free staples, as presented in Figure 3A. This suggests that, in contrast with Mg^{2+} (Figure S2), nonspecifically adsorbed DNA staples and scaffolds can be mostly eliminated from the surface prepared by Na^+ during surface deposition. It may be surprising that the adsorption of free thiolated staples is so low in Na^+ buffer even without a purification step. Our previous studies showed that insertion of thiolated DNA into MUDA SAMs in a similar buffer is slow.[9] Even when the concentration of thiolated DNA is 100 nM, the density of inserted DNA is only about 1.33×10^{10} /cm^2 ($1.33/100 \times 100$ nm^2). As the total concentration of the thiolated staples is only 50 nM in this study, the density of deposited DNA staples is only even lower, 0.28×10^{10} staples/cm^2 ($0.28/100 \times 100$ nm^2). In contrast, the DNA origami stamps confine the thiolated staples to the surface and substantially accelerate the insertion process. Therefore, the insertion of free staples only account for ~8% of the overall surface features when deposited under Na^+(Figure 3A).

To expose the spatial patterns of the transferred ink molecules, DNA origami nanostructure was denatured in 100% formamide and rinsed with a STAE buffer, triggering the removal of the DNA origami frame (*i.e.*, non-thiolated staples and scaffold). AFM shows that while the DNA origami features disappeared, surface-anchored staples remained on the surface after the denaturing step, as indicated by the dot-like features in Figure 3B. In contrast, the same dot-like features were not observed in a control experiment using non-thiolated staples (Figure 2C), confirming that the surface-tethered staples shown in Figure 3B were transferred from DNA mini-tiles due to the strong gold-thiol interactions (Figure 3A). It should be pointed out that, so far, the characterizations of the transferred single molecule patterns rely on further conjugation with reporters such as dyes,[40-41] proteins[32, 42] and AuNPs.[20, 28, 40-41, 43] Thus the reliability of characterization may be diminished by nonspecific adsorption of these reporters. Our single-molecule AFM imaging technique,[34] on the other hand, makes it possible to directly visualize the transferred DNA molecules without reporter labelling. Since nonspecific adsorption is mostly absent on the surface (Figure 3A), we incorporated single molecule spatial statistical analysis developed in our prior work to assess the spatial patterns of printed single molecules.[8-9] Notably, the transferred staples were identified and selected from the features with height between 0.4 and 2.4 nm in AFM images (see Materials and Methods section for details). As depicted in Figure 4A, spatial statistical analysis of the staple surface prepared by DNA origami nanostructure (Figure 3B) yields a mean nearest neighbor distance (NND, the distance between a staple and its closest neighbor) of 12.4 nm that is comparable to the expected separation distance of about 10.3 nm for a pair of thiolated staples (Figure 1A), considering the existence of a small fraction of immobilized free staples (~8% of the overall surface features in Figure 3A). In contrast, a surface prepared by direct insertion of thiolated staples into a MUDA SAM exhibited a random distribution with a mean NND of 26.7 nm (Figure 3C and 4B). Moreover, the fraction of staples with NND ranging from 5 nm to 15 nm (a range that is close to the designed distance of 10.3 nm in Figure 1A), is about 66% under nanoimprinting (Figure 4A) and only 8% under direct insertion (Figure 4B). The former is the consequence of dimer formation, while the latter arises from random distribution of inserted staples. Additionally, we analyzed the NNDs of randomly generated coordinates of DNAs with the same overall density (Figure 4C). The experimental and simulated distributions (Figure 4B and 4C) are remarkably similar, in agreement with our earlier studies showing that the direct insertion process immobilizes thiolated DNA to the gold surface in a mostly random fashion.[9, 31] The minor difference is that the simulated distribution has more molecules with NNDs less than 15 nm, which suggests that repulsive interactions between DNAs disfavor DNAs to be inserted in close proximity. From Monte Carlo simulation of 5000 images, we were able to extract the histogram of the fraction of NNDs falling in between 5-15 nm (Figure S3). The histogram is found to follow a normal distribution, 0.30 ± 0.04. From this distribution, we calculate the probability of observing 66% or more of NNDs between 5-15 nm to be close to zero (3.9×10^{-13}). Considering the repulsive interactions between the DNA staples, the probability of observing so many molecules with such small NNDs

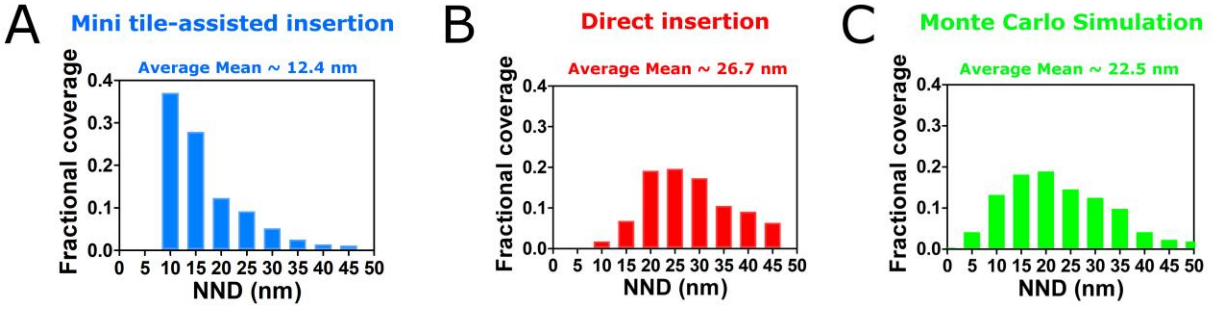

Figure 4. Spatial statistical analysis of the surface-immobilized staples. The nearest-neighbor distance (NND) analysis of the inserted staples using (A) DNA mini-tile-assisted nanoimprinting (Figure 3B) and (B) direct insertion (Figure 3C). (C) The NND distribution under complete spatial randomness generated using Monte Carlo simulation. The NNDs were sorted into bins to form histogram with a bin width of 5 nm, *i.e.* ± 2.5 nm with respect to the center value of the bins.

should be even smaller. Therefore, the non-random distribution of NNDs of the thiolated DNAs via DNA origami assisted insertion (Figure 4A) shows that the DNA origami template is responsible for placing these DNA ink molecules in spatial proximity. These values allow us to calculate the yield of transferring a single ink molecule through the insertion approach. The fractions of DNA origami nanostamps that transfer a dimer, monomer, or no staple are χ_{dim}, χ_{mon}, $\chi_{notrans}$, respectively. The fraction of nonspecifically deposited staples is $\chi_{nonspecific} = 0.08$.

$$\chi_{dim} + \chi_{mon} + \chi_{notrans} + \chi_{nonspecific} = 1 \quad (1)$$

After denaturing, the molecules that form a dimer make up 66% of the observed single molecule features:

$$2\chi_{dim} / (2\chi_{dim} + \chi_{mon} + \chi_{nonspecific}) = 0.66 \quad (2)$$

If we assume that the transfers of the two ink molecules from a stamp to the surface are independent and the two ink molecules have an identical transfer yield Y_{ink}, $\chi_{dim} : \chi_{mon} : \chi_{notrans}$ should follow the binomial distribution:

$$\chi_{dim} : \chi_{mon} : \chi_{notrans} = Y_{ink}^2 : 2Y_{ink}(1\text{-}Y_{ink}) : (1\text{-}Y_{ink})^2 \quad (3)$$

By combining (1)-(3), Y_{ink} is calculated to be 0.7, which is almost identical to the estimated value in a previous DNA origami imprinting study.[28] While one might assume that our new method, which relies on the insertion of thiolated staples into the defects or replacing pre-existing thiol molecules on a highly ordered SAM, may be less efficient than the existing method that transfers ink molecules to a bare gold substrate, the yield achieved suggests that the confinement of thiolated staples between the DNA origami stamp and SAM substantially accelerates the insertion process and leads to a good transfer yield. Moreover, our approach obviates the need for a separate step for surface passivation after ink transfer,[28] which likely reduces Y_{ink} due to desorption and lateral diffusion of the ink molecules.

Finally, a fraction of tiles may be deposited on the surface with the side of the thiolated staples facing up and therefore do not lead to gold-thiol bond formation. To assess the deposition orientation of the tiles, we compared the tile surface density before denaturation with the density of single molecules after denaturation. The tile surface density of 3.5×10^{10} tiles/cm^2 ($3.5 / 100 \times 100$ nm^2) before denaturation (Figure 3A) would lead to an ink molecule surface density of 4.9×10^{10} /cm^2 ($4.9 / 100 \times 100$ nm^2) if all tiles were deposited on surface with the side with the thiolated staples facing down with a transfer yield of 70%. In addition to the printed ink molecules, the surface also contains about $0.3\text{-}0.4 \times 10^{10}$ /cm^2 ($0.3\text{-}0.4 / 100 \times 100$ nm^2) nonspecifically adsorbed staples. Therefore, the observed density of 5.4×10^{10} /cm^2 ($5.4 / 100 \times 100$ nm^2) after denaturation (Figure 3B) suggests two likely scenarios. In the first scenario, only a small fraction of tiles with the protruding thiolated staples are deposited with the ink molecule side facing away from the SAM and the ink molecules can only be transferred when the ink molecule side is direct contact with the SAM. Indeed, a recent study by Gopinath et al. showed that the flat side, *i.e.*, the side without protruding staples, is more likely be deposited onto the surface than the side with protruding staples as the flat side can form intimate contact with the solid surface.[44] In the second scenario, thiolated staples that are oriented away from the surface can also be transferred to the solid support. Although this scenario has not been considered in previous studies,[28, 32] it cannot be excluded as the mercapto-hexyl tether may penetrate the gap between the helices of the DNA origami tile and insert itself into the SAM due to the flexibility of the staple extension and small cross section of the tether (~0.5 nm). Future experiments that print asymmetric staple patterns will help elucidate the mechanism of ink molecule transfer.

CONCLUSIONS

In summary, we have developed a DNA-origami-nanostructure-based nanopatterning method that imprints single thiolated oligonucleotides (ink molecules) onto a highly ordered SAM on gold. This simple method minimizes the nonspecific binding of DNA components to the surface and enables high resolution, label-free characterization of the spatial arrangement of individual ink molecules as well as determination of ink transfer yield. The ink transfer yield achieved is comparable to the best achieved in the literature.[28] A limitation that is common to all existing DNA origami nanoimprinting studies is that the ink transfer yield remains inadequate for printing complex single molecule patterns with a practical yield. Even with the best currently available ink transfer yield of 70%, a trimer design would have a yield of only 34% and the yield of an octamer design is 6%, which would be too low for many potential applications. Nevertheless, with the ability to image the single molecule patterns without the use of labels, our approach offers a pathway toward improving the ink transfer yield and ultimately the printing of more complex single molecule patterns. We expect that improved purification of the DNA origami stamp and optimization of the deposition condition can further improve the yield and allow the patterning of more complex single molecule patterns. Once the yield is further improved, our approach should be ideally suited for producing single molecule nanoarrays for multiplex detection of biomarkers. First of all, as the ink molecules transferred from a single stamp have different sequences, different biomarkers such as nucleic acids[9] or even aptamer-binding proteins[45] can be selectively captured by the ink molecules. Second, the binding of biomarkers can be read out using high resolution microscopy techniques without the use of labels.[9, 34, 37] Third, patterns printed on a passivated surface can be readily used for biomarker detection. In contrast, approaches that print ink molecules directly onto a gold surface would require another step of surface passivation to suppress nonspecific adsorption of biomolecules, which may disrupt the patterns.[28] These single molecule patterns printed on a passivated surface may serve as a powerful tool to elucidate the structure-function relationship of interfacial molecular recognition in both biological systems[5-7] and biotechnological devices.[8-9] For example, this method may be used to investigate the molecular crowding effect on hybridization by systematically varying the intermolecular separations,[20, 46-50] which can be realized by changing the positions and the number of modified staples on DNA origami nanostructure. Our approach may also allow the formation of designed single molecule patterns of ligands/receptors on solid supports to study cell-surface interactions that are important in a host of biological phenomena, from cell proliferation,[6] differentiation,[51] apoptosis[52] to immune response.[7, 53]

MATERIALS AND METHODS

Materials. Both thiolated and unmodified oligonucleotide staples shown in Table S1 were ordered from IDT (Coralville, IA, USA) and used as received. M13mp18 RF I phage vector, pTXB1 vector, all enzymes and buffers used in template linearization, digestion of complementary DNA strands and polymerase chain reaction (PCR) were purchased from New England Biolabs Inc. (Ipswich, MA, USA). QIAquick PCR Purification Kit was obtained from Qiagen (Valencia, CA, USA). 11-mercaptoundecanoic acid (MUDA,

≥98%) and Tris-(2-carboxyethyl) phosphate (TCEP, ≥98%) were all obtained from Sigma-Aldrich (St. Louis, MI, USA). All chemicals were acquired from Fisher Scientific (Pittsburgh, PA, USA) and used without further purification, unless noted otherwise. Gold wires with 99.99% purity and a diameter of 1 mm were purchased from Scientific Instrument Service (Ringoes, NJ, USA). Amicon centrifugal filters and Freeze-Squeeze columns were purchased from Millipore (Billerica, MA, USA) and Biorad (Hercules, CA, USA) respectively. All glassware was cleaned with piranha solution (4:1 sulfuric acid:hydrogen peroxide) and thoroughly rinsed with ultrapure DI water before use. **CAUTION**: piranha is highly reactive and corrosive and should be stored in open containers in a fume hood. Mixing piranha with organic materials can result in explosion and should be handled with extreme care. Protective goggles and gloves must be used during operation.

Generation of Mini-Scaffolds. A solution of 10 ng/μL circular M13mp18 RF I, 20 units of EcoRI enzyme, 200 μg/μL BSA, and 1× EcoRI buffer was incubated at 37 °C for 2 h to linearize the phage vector, heated up to 65 °C for 20 min to denature the enzymes, followed by cooling at 4 °C in a thermal cycler. After linearization, M13mp18 RF I were purified with the Qiagen QIAquick PCR Purification Kit. Following purification, 50 pg/μL of linearized M13mp18 RF I was mixed with 200 nM of forward/reverse primers and OneTaq 1× master mix with standard buffer. The following protocol was used for PCR amplification of the dsDNA scaffolds: an initial denaturation of 95 °C for 3 min, followed by 34 repeating cycles of 95°C for 3 s, 53°C for 45 s, 72°C for 2 min 30 s, a final 10 min extension at 72 °C, followed by cooling at 4 °C. The amplified scaffolds were purified with the Qiagen QIAquick PCR Purification Kit. To remove complementary DNA strands from PCR-amplified dsDNA scaffolds, a solution of ~30 nM dsDNA scaffolds, 40 units of lambda exonuclease, and 1 × lambda exonuclease reaction was incubated at 37 °C for 6 h to digest the complementary strands, heated up to 75 °C for 10 min to denature the enzymes, followed by cooling at 4 °C. The enzyme-digested ssDNA scaffolds were then purified with the Qiagen QIAquick PCR Purification Kit.

DNA Origami Nanostructure Folding and Purification. DNA origami folding was carried out by incubating a solution of 5 nM DNA mini-scaffold, 25 nM for each DNA staple, 1× TAE and 12.5 mM $MgAc_2$ (or 1M NaAc) according to the following annealing protocol: 90°C for 5 min and controlled cooling from 90°C to 20°C at a cooling rate of 1°C/min.[28, 37] The assembled DNA origami nanostructures were then purified using Amicon centrifugal filters or gel purification.

Preparation of 11-Mercaptoundecanoic Acid (MUDA) Functionalized Gold Surface. The Au (111) facets on a small single-crystal gold bead were prepared by melting one end of the gold wire (99.99% in purity) following Clavilier's method[54] and used as substrates for SAM formation. The gold bead was cleaned before use by a 15-min immersion in hot nitric acid solution, followed by hydrogen flame annealing. The MUDA SAM was formed by incubating the cleaned gold bead in 1 mM MUDA dissolved in 9:1 (v/v) ethanol:acetic acid overnight. Before the deposition of DNA origami nanostructures, the gold bead was sonicated in an ethanolic solution that contains 10% (v/v) of acetic acid and then rinsed with ultrapure DI water.

DNA Origami Deposition and Denaturation. DNA origami solution containing 1× TAE, 12.5 mM $MgAc_2$ (or 1M NaAc) and 1 mM TCEP was deposited onto the gold bead passivated with MUDA SAM for 1 hr at room temperature. The gold bead was then rinsed 3 times with STAE buffer (1× TAE, 200 mM NaAc) to remove the unbound origami assembly. The surface-tethered DNA origami nanostructures were denatured by immersing the gold bead in 100% formamide at room temperature. After denaturation, the gold bead was rinsed out with ultrapure DI water to expose the surface-tethered staples.

Gel Extraction of DNA Origami. The folded DNA origami nanostructures were loaded into a 1% SYBR Green I stained agarose gel submerged in a running buffer of 0.5× TBE (45 mM Tris base, 45 mM boric acid, 1 mM EDTA, pH 8.0). A constant voltage of 65 V was applied for 1 hr. The bands of interest in the agarose were cut out and trimmed. The trimmed gel slices were chopped and placed into the Freeze-Squeeze columns to extract the folded DNA origami nanostructures.

AFM Characterization. All imaging was carried out using Agilent technologies 5500 AFM manufactured by Keysight Technologies (Santa Rosa, CA, USA). AFM images were acquired while operating in tapping mode under an aqueous Ni^{2+} imaging buffer (5 mM $NiAc_2$, 0.1× TAE), using silicon tips mounted on silicon nitride cantilevers with a nominal spring constant of ~0.2-0.4 N/m and a resonant frequency of approximately 15 kHz in liquid (model SNL-10, manufactured by Bruker, Billerica, MA, USA).

Spatial Statistical Analysis of Surface-Tethered Staples. All statistics used in this study were obtained from at least 4 AFM images acquired on the same sample surface. AFM images were processed using Gwyddion open-source software. The XY spatial coordinates of the surface-bound staples were measured and used to calculate the nearest neighbor distance (NND). Individual staples were identified after first flattening AFM images line by line, then masking staples using Gwyddion software (http://gwyddion.net/). After line-by-line flattening, a mask was generated for all features that are over a minimum height threshold of 0.4 nm and below a maximum height threshold of 2.4 nm. Minor manual editing was carried out to separate the partially overlapping features, especially for areas at higher staple densities. The heights of the individual staples were then recorded relative to the mean height of a ten-pixel halo immediately surrounding that staple.

ASSOCIATED CONTENT

Supporting Information

This material is available free of charge at

A list of all DNA oligonucleotides used, gel images of DNA origami nanostructures, AFM images of DNA origami nanostructures folded under Mg^{2+}, images of Monte Carlo simulated distribution of staples, and probability distribution of fractions of staples with NND ranging from 5 nm to 15 nm (PDF)

ACKNOWLEDGMENTS

This work was financially supported by Department of Energy (DE-SC0020961) and National Science Foundation (CHE-1808213), Q.G. was supported by Graduate Dean's Dissertation Fellowship and UC Merced MBSE Bobcat Fellowship.

REFERENCES

(1) Lee, K. B.; Park, S. J.; Mirkin, C. A.; Smith, J. C.; Mrksich, M., Protein Nanoarrays Generated by Dip-Pen Nanolithography. *Science* **2002,** *295* (5560), 1702-1705.

(2) Kilian, K. A.; Bugarija, B.; Lahn, B. T.; Mrksich, M., Geometric Cues for Directing the Differentiation of Mesenchymal Stem Cells. *Proc. Natl. Acad. Sci. USA* **2010,** *107* (11), 4872-4877.

(3) Liu, Y.; Wang, K.; Chen, H.; Li, J.; Laurence, T. A.; Ly, S.; Liu, F.; Liu, G., Periodic Arrangement of Lipopolysaccharides Nanostructures Accelerates and Enhances the Maturation Processe of Dendritic Cells. *ACS Appl. Nano Mater.* **2018**, *1* (2), 839−850.
(4) Howorka, S.; Hesse, J., Microarrays and Single Molecules: An Exciting Combination. *Soft Matter* **2014,** *10* (7), 931-941.
(5) Fu, J.; Liu, M.; Liu, Y.; Woodbury, N. W.; Yan, H., Interenzyme Substrate Diffusion for an Enzyme Cascade Organized on Spatially Addressable DNA Nanostructures. *J. Am. Chem. Soc.* **2012,** *134* (12), 5516-5519.
(6) Cavalcanti-Adam, E. A.; Volberg, T.; Micoulet, A.; Kessler, H.; Geiger, B.; Spatz, J. P., Cell Spreading and Focal Adhesion Dynamics Are Regulated by Spacing of Integrin Ligands. *Biophys. J.* **2007,** *92* (8), 2964-2974.
(7) Vorup-Jensen, T., On the Roles of Polyvalent Binding in Immune Recognition: Perspectives in the Nanoscience of Immunology and the Immune Response to Nanomedicines. *Adv. Drug Deliv. Rev.* **2012,** *64* (15), 1759-1781.
(8) Gu, Q.; Cao, H. H.; Zhang, Y.; Wang, H.; Petrek, Z. J.; Shi, F.; Josephs, E. A.; Ye, T., Toward a Quantitative Relationship between Nanoscale Spatial Organization and Hybridization Kinetics of Surface Immobilized Hairpin DNA Probes. *ACS Sens.* **2020**, *6* (2), 371-379.
(9) Gu, Q.; Nanney, W.; Cao, H. H.; Wang, H.; Ye, T., Single Molecule Profiling of Molecular Recognition at a Model Electrochemical Biosensor. *J. Am. Chem. Soc.* **2018,** *140* (43), 14134-14143.
(10) Pei, H.; Lu, N.; Wen, Y. L.; Song, S. P.; Liu, Y.; Yan, H.; Fan, C. H., A DNA Nanostructure-Based Biomolecular Probe Carrier Platform for Electrochemical Biosensing. *Adv. Mater.* **2010,** *22* (42), 4754-4758.
(11) Kufer, S. K.; Puchner, E. M.; Gumpp, H.; Liedl, T.; Gaub, H. E., Single-Molecule Cut-and-Paste Surface Assembly. *Science* **2008,** *319* (5863), 594-596.
(12) Hao, X.; Josephs, E. A.; Gu, Q.; Ye, T., Molecular Conformations of DNA Targets Captured by Model Nanoarrays. *Nanoscale* **2017,** *9* (36), 13419-13424.
(13) Fan, S.; Wang, D.; Kenaan, A.; Cheng, J.; Cui, D.; Song, J., Create Nanoscale Patterns with DNA Origami. *Small* **2019,** *15* (26), 1805554.
(14) Hong, F.; Zhang, F.; Liu, Y.; Yan, H., DNA Origami: Scaffolds for Creating Higher Order Structures. *Chem. Rev.* **2017,** *117* (20), 12584-12640.
(15) Du, K.; Park, M.; Ding, J.; Hu, H.; Zhang, Z., Sub-10 nm Patterning with DNA Nanostructures: A Short Perspective. *Nanotechnology* **2017,** *28* (44), 442501.
(16) Johnson-Buck, A.; Nangreave, J.; Jiang, S.; Yan, H.; Walter, N. G., Multifactorial Modulation of Binding and Dissociation Kinetics on Two-Dimensional DNA Nanostructures. *Nano Lett.* **2013,** *13* (6), 2754-2759.
(17) Kong, G.; Xiong, M.; Liu, L.; Hu, L.; Meng, H. M.; Ke, G.; Zhang, X. B.; Tan, W., DNA Origami-Based Protein Networks: From Basic Construction to Emerging Applications. *Chem. Soc. Rev.* **2020**, *50*, 1846-1873.
(18) Kielar, C.; Reddavide, F. V.; Tubbenhauer, S.; Cui, M.; Xu, X.; Grundmeier, G.; Zhang, Y.; Keller, A., Pharmacophore Nanoarrays on DNA Origami Substrates as a Single-Molecule Assay for Fragment-Based Drug Discovery. *Angew. Chem. Int. Ed.* **2018,** *57* (45), 14873-14877.
(19) Huang, J.; Suma, A.; Cui, M.; Grundmeier, G.; Carnevale, V.; Zhang, Y.; Kielar, C.; Keller, A., Arranging Small Molecules with Subnanometer Precision on DNA Origami Substrates for the Single-Molecule Investigation of Protein-Ligand Interactions. *Small Struct.* **2020**, *1*, 2000038.
(20) Lin, M.; Wang, J.; Zhou, G.; Wang, J.; Wu, N.; Lu, J.; Gao, J.; Chen, X.; Shi, J.; Zuo, X.; Fan, C., Programmable Engineering of a Biosensing Interface with Tetrahedral DNA Nanostructures for Ultrasensitive DNA Detection. *Angew. Chem. Int. Ed.* **2015,** *54* (7), 2151-2155.
(21) Shen, C.; Lan, X.; Lu, X.; Meyer, T. A.; Ni, W.; Ke, Y.; Wang, Q., Site-Specific Surface Functionalization of Gold Nanorods Using DNA Origami Clamps. *J. Am. Chem. Soc.* **2016,** *138* (6), 1764-1767.
(22) Shen, J.; Tang, Q.; Li, L.; Li, J.; Zuo, X.; Qu, X.; Pei, H.; Wang, L.; Fan, C., Valence-Engineering of Quantum Dots Using Programmable DNA Scaffolds. *Angew. Chem. Int. Ed.* **2017,** *56* (50), 16077-16081.
(23) Hannewald, N.; Winterwerber, P.; Zechel, S.; Ng, D. Y. W.; Hager, M. D.; Weil, T.; Schubert, U. S., DNA Origami Meets Polymers: A Powerful Tool for the Design of Defined Nanostructures. *Angew. Chem. Int. Ed.* **2020**, *60* (12), 6218-6229.
(24) Mei, Q.; Wei, X.; Su, F.; Liu, Y.; Youngbull, C.; Johnson, R.; Lindsay, S.; Yan, H.; Meldrum, D., Stability of DNA Origami Nanoarrays in Cell Lysate. *Nano Lett.* **2011,** *11* (4), 1477-1482.
(25) Stephanopoulos, N., Strategies for Stabilizing DNA Nanostructures to Biological Conditions. *Chem. Bio. Chem.* **2019,** *20* (17), 2191-2197.
(26) Bila, H.; Kurisinkal, E. E.; Bastings, M. M. C., Engineering a Stable Future for DNA-Origami as a Biomaterial. *Biomater. Sci.* **2019,** *7* (2), 532-541.
(27) Ramakrishnan, S.; Ijas, H.; Linko, V.; Keller, A., Structural Stability of DNA Origami Nanostructures under Application-Specific Conditions. *Comput. Struct. Biotechnol. J.* **2018,** *16*, 342-349.
(28) Gallego, I.; Manning, B.; Prades, J. D.; Mir, M.; Samitier, J.; Eritja, R., DNA-Origami-Driven Lithography for Patterning on Gold Surfaces with Sub-10 nm Resolution. *Adv. Mater.* **2017,** *29* (11), 1603233.
(29) Vericat, C.; Vela, M. E.; Benitez, G.; Carro, P.; Salvarezza, R. C., Self-Assembled Monolayers of Thiols and Dithiols on Gold: New Challenges for a Well-Known System. *Chem. Soc. Rev.* **2010,** *39* (5), 1805-1834.
(30) Herne, T. M.; Tarlov, M. J., Characterization of DNA Probes Immobilized on Gold Surfaces. *J. Am. Chem. Soc.* **1997,** *119* (38), 8916-8920.
(31) Josephs, E. A.; Ye, T., Nanoscale Spatial Distribution of Thiolated DNA on Model Nucleic Acid Sensor Surfaces. *ACS Nano* **2013,** *7* (4), 3653-3660.
(32) Sajfutdinow, M.; Uhlig, K.; Prager, A.; Schneider, C.; Abel, B.; Smith, D. M., Nanoscale Patterning of Self-Assembled Monolayer (SAM)-Functionalized Substrates with Single Molecule Contact Printing. *Nanoscale* **2017,** *9* (39), 15098-15106.
(33) Shuster, M. J.; Vaish, A.; Cao, H. H.; Guttentag, A. I.; McManigle, J. E.; Gibb, A. L.; Martinez-Rivera, M.; Nezarati, R. M.; Hinds, J. M.; Liao, W. S.; Weiss, P. S.; Andrews, A. M., Patterning Small-Molecule Biocapture Surfaces: Microcontact Insertion Printing Vs. Photolithography. *Chem. Commun.* **2011,** *47* (38), 10641-10643.
(34) Abel, G. R., Jr.; Josephs, E. A.; Luong, N.; Ye, T., A Switchable Surface Enables Visualization of Single DNA Hybridization Events with Atomic Force Microscopy. *J. Am. Chem. Soc.* **2013,** *135* (17), 6399-6402.
(35) Hansma, H. G.; Laney, D. E., DNA Binding to Mica Correlates with Cationic Radius: Assay by Atomic Force Microscopy. *Biophys. J.* **1996,** *70* (4), 1933-1939.
(36) Aghebat Rafat, A.; Pirzer, T.; Scheible, M. B.; Kostina, A.; Simmel, F. C., Surface-Assisted Large-Scale Ordering of DNA Origami Tiles. *Angew. Chem. Int. Ed.* **2014,** *53* (29), 7665-7668.
(37) Cao, H. H.; Abel, G. R., Jr.; Gu, Q.; Gueorguieva, G. V.; Zhang, Y.; Nanney, W. A.; Provencio, E. T.; Ye, T., Seeding the Self-Assembly of DNA Origamis at Surfaces. *ACS Nano* **2020,** *14* (5), 5203-5212.
(38) Woo, S.; Rothemund, P. W., Self-Assembly of Two-Dimensional DNA Origami Lattices Using Cation-Controlled Surface Diffusion. *Nat. Commun.* **2014,** *5*, 4889.
(39) Martin, T. G.; Dietz, H., Magnesium-Free Self-Assembly of Multi-Layer DNA Objects. *Nat. Commun.* **2012,** *3*, 1103.
(40) Edwardson, T. G.; Lau, K. L.; Bousmail, D.; Serpell, C. J.; Sleiman, H. F., Transfer of Molecular Recognition Information from DNA Nanostructures to Gold Nanoparticles. *Nat. Chem.* **2016,** *8* (2), 162-170.
(41) Xie, N.; Liu, S.; Fang, H.; Yang, Y.; Quan, K.; Li, J.; Yang, X.; Wang, K.; Huang, J., Three-Dimensional Molecular Transfer from DNA Nanocages to Inner Gold Nanoparticle Surfaces. *ACS Nano* **2019,** *13* (4), 4174-4182.
(42) Busuttil, K.; Rotaru, A.; Dong, M.; Besenbacher, F.; Gothelf, K. V., Transfer of a Protein Pattern from Self-Assembled DNA Origami to a Functionalized Substrate. *Chem. Commun.* **2013,** *49* (19), 1927-1929.
(43) Daems, D.; Pfeifer, W.; Rutten, I.; Sacca, B.; Spasic, D.; Lammertyn, J., Three-Dimensional DNA Origami as Programmable Anchoring Points for Bioreceptors in Fiber Optic Surface Plasmon Resonance Biosensing. *ACS Appl. Mater. Interfaces* **2018,** *10* (28), 23539-23547.
(44) Gopinath, A.; Thachuk, C.; Mitskovets, A.; Atwater, H. A.; Kirkpatrick, D.; Rothemund, P. W. K., Absolute and Arbitrary Orientation of Single-Molecule Shapes. *Science* **2021,** *371* (6531), eabd6179
(45) Xiao, Y.; Lubin, A. A.; Heeger, A. J.; Plaxco, K. W., Label-Free Electronic Detection of Thrombin in Blood Serum by Using an Aptamer-Based Sensor. *Angew. Chem. Int. Ed.* **2005,** *44* (34), 5456-5459.
(46) Ricci, F.; Lai, R. Y.; Heeger, A. J.; Plaxco, K. W.; Sumner, J. J., Effect of Molecular Crowding on the Response of an Electrochemical DNA Sensor. *Langmuir* **2007,** *23* (12), 6827-6834.
(47) Cederquist, K. B.; Golightly, R. S.; Keating, C. D., Molecular Beacon-Metal Nanowire Interface: Effect of Probe Sequence and Surface Coverage on Sensor Performance. *Langmuir* **2008,** *24* (16), 9162-9171.
(48) Cederquist, K. B.; Keating, C. D., Hybridization Efficiency of Molecular Beacons Bound to Gold Nanowires: Effect of Surface Coverage and Target Length. *Langmuir* **2010,** *26* (23), 18273-18280.
(49) Morrin, G. M.; Schwartz, D. K., Three Regimes of Polymer Surface Dynamics under Crowded Conditions. *Macromolecules* **2018,** *51* (3), 1207-1214.

(50) Peterson, A. W.; Heaton, R. J.; Georgiadis, R. M., The Effect of Surface Probe Density on DNA Hybridization. *Nucleic Acids Res.* **2001,** *29* (24), 5163-5168.
(51) Stephanopoulos, N.; Freeman, R.; North, H. A.; Sur, S.; Jeong, S. J.; Tantakitti, F.; Kessler, J. A.; Stupp, S. I., Bioactive DNA-Peptide Nanotubes Enhance the Differentiation of Neural Stem Cells into Neurons. *Nano Lett.* **2015,** *15* (1), 603-609.
(52) Wang, Y.; Baars, I.; Fordos, F.; Hogberg, B., Clustering of Death Receptor for Apoptosis Using Nanoscale Patterns of Peptides. *ACS Nano* **2021**, *15* (6), 9614-9626.
(53) Fallarini, S.; Paoletti, T.; Battaglini, C. O.; Ronchi, P.; Lay, L.; Bonomi, R.; Jha, S.; Mancin, F.; Scrimin, P.; Lombardi, G., Factors Affecting T Cell Responses Induced by Fully Synthetic Glyco-Gold-Nanoparticles. *Nanoscale* **2013,** *5* (1), 390-400.
(54) Clavilier, J.; Faure, R.; Guinet, G.; Durand, R., Preparation of Mono-Crystalline Pt Microelectrodes and Electrochemical Study of the Plane Surfaces Cut in the Direction of the (111) and (110) Planes. *J. Electroanal. Chem.* **1980**, *107* (1), 205-209.